SPE-191971-MS

# Enhanced Oil Recovery by Nanoparticle-Induced Crude Oil Swelling: Pore-Scale Experiments and Understanding

Devesh Agrawal, Ke Xu, Qusai Darugar, and Valery Khabashesku, Baker Hughes, a GE Company



This paper was prepared for presentation at the SPE Asia Pacific Oil & Gas Conference and Exhibition held in Brisbane, Australia, 23–25 October 2018.





## Abstract

Nanoparticle (NP) based enhanced oil recovery (Nano-EOR) has been considered as a promising future EOR strategy. However, although many mechanisms of Nano-EOR have been proposed, a lack of direct connections between the pore-scale mechanisms and the macro-scale oil recovery performance makes it hard to determine which mechanisms are dominant. In this work, we discovered a novel phenomenon of nanoparticle-crude oil interaction in pore-scale. Multi-scale experiments were conducted to connect this novel pore-scale phenomenon's role to oil recovery performance.

A microchannel with dead-end pore was used to observe crude oil-NP interactions, on which crude oil can be trapped in the dead-end pore with a stable crude oil-aqueous phase interface at the pore-throat. A glass porous micromodel was used to conduct oil displacement experiments. ASW was used as the secondary flooding fluid, and 2000 PPM negatively charged NP in ASW was applied as the tertiary flooding fluid. Saturation profiles were recorded and analyzed by advanced image analysis tools. A coreflood through the sandstone sample was also conducted with similar conditions to the micromodel-flood experiments.

A phenomenon that has never been reported was observed from the dead-end pore microchannel. It was observed that crude oil can considerably swell when contacting the nanoparticle aqueous suspension. In an ideal case (5 wt% NP in DI water), the oil volume more than doubled after a 50-hour swelling. The possible explanation for the crude oil swelling could be spontaneous formation of water droplets in the crude oil phase. NP can very likely affect the distribution of natural surfactants in crude oil (on the interface or inside oil phase), which breaks the water balance between aqueous phase and crude oil. This view has received support from quantitative experiments. It was shown from 2.5 D micromodel flood experiments that 11.8% incremental oil recovery comes slowly and continuously in more than 20 hours (40 pore volumes). From a saturation profile analysis, swelling of crude oil was found to improve sweep efficiency. Coreflood experiments also showed that the incremental oil was slowly and continuously recovered in about 20 hours during NP flooding. We propose that reduction of local water mobility by oil swelling in the swept region is the mechanism of sweep efficiency improvement.

Swelling of crude oil under a NP environment was observed for the first time, with a systematic theory proposed and examined by quantitative experiments. The micromodel flood and coreflood experiments showed slow incremental oil recovery with a similar time scale to the oil swelling. Image analysis on the

micromodel flood demonstrated improvement in the sweep efficiency during NP flooding. The mechanism for this sweep improvement is proposed.

**Keywords:** Nanoparticle, Enhanced Oil Recovery, Crude Oil Swelling, Micromodel

## Introduction

Global demand for crude oil is continuously increasing[1]. Current crude oil recovery from reservoirs using existing technologies is not satisfactory and depending upon reservoir characteristics, on an average over 50 % of the crude oil is not ecovered from a reservoir[2]. In the last several decades, several enhanced oil recovery (EOR) methods have been investigated in laboratories and proposed for field-scale implementations[3]. Most commonly and widely studied EOR methods are based on use of surfactants, polymers, alkalis and their combinations as injection fluids for enhancing oil recovery[4,5,6]. Conventional methods have advantages over any new methods because mechanisms of crude-oil recovery are investigated in great detail, fields know-how are also understood to some extent and numerous field case-studies and production results are available[7,8,9]. EOR surfactants work on the principle of reducing interfacial tension (IFT) between crude oil and water which helps to increase capillary number and reduce residual crude oil saturation. Similarly, polymer also helps to increase capillary number by increasing the viscosity of the injected fluid which ultimately improves sweep efficiency of the flooding process. However, conventional methods are not entirely adequate due to poor recovery efficiency, high cost of chemical injection primarily due to shear degradation and excessive adsorption on rock matrix. Hence, more efficient and economic EOR method is urgently needed in the Oil & Gas industry.

Nanoparticle (NP) based enhanced oil recovery (Nano-EOR) has been considered as a promising future EOR strategy. Nanoparticles due to small size (typically at least one dimension 1-100 nanometers), very high surface area (~$10^2$ meter$^2$ per gram) and very high surface charge density hold very promising potential in increasing crude oil recovery efficiency at lower concentrations than the conventionally used chemicals. Researchers globally have been studying all kinds of nanoparticles such as $Al_2O_3$, CuO, $Fe_2O_3$/$Fe_3O_4$, $Ni_2O_3$, MgO, $SnO_2$, $TiO_2$, ZnO, $ZrO_2$, SiO2, carbon nanoparticles, and carbon nanotubes for assessing their potential in EOR. Sustained efforts in last several years have resulted in the discovery of several novel EOR mechanisms for Nano-EOR such as: disjoining pressure[10,11], log-jamming[12], wettability alteration, reduction of interfacial tension (IFT), viscosity enhancement and crude oil viscosity reduction[13]. Unlike surfactants and polymers, it is quite evident that there is no single universally accepted mechanism for nanoparticles enabled EOR. Although many mechanisms of Nano-EOR have been proposed, a lack of direct connections between the pore-scale mechanisms and the macro-scale oil recovery performance makes it hard to determine which mechanisms are dominant. Nanoparticles are also increasingly studied for addressing key challenges to supplement conventional EOR methods by reducing surfactants adsorption[14], increasing polymer viscosity and reduce shear degradation. Therefore, it is important that mechanism for nanoparticle enabled recovery be identified and pore-scale physics be validated and expanded in the pore-networks on the micro-model, and finally performance and physics be validated in the reservoir core.

In this work, we have discovered a novel phenomenon of nanoparticle-crude oil interaction at pore-scale. Multi-scale experiments were conducted to connect this novel pore-scale phenomenon's role in oil recovery performance. Pore-scale (~$10^{-4}$ m) study was conducted on dead-end-pore micro-channnel pore scale physics was identified, which was further expanded in the pore-networks on 2.5 D micromodel chip (~$10^{-1}$ m) and performance was validated in the core-scale inside an outcropped Idaho Gray core (~$10^{-1}$ m) on core-flooding setup.

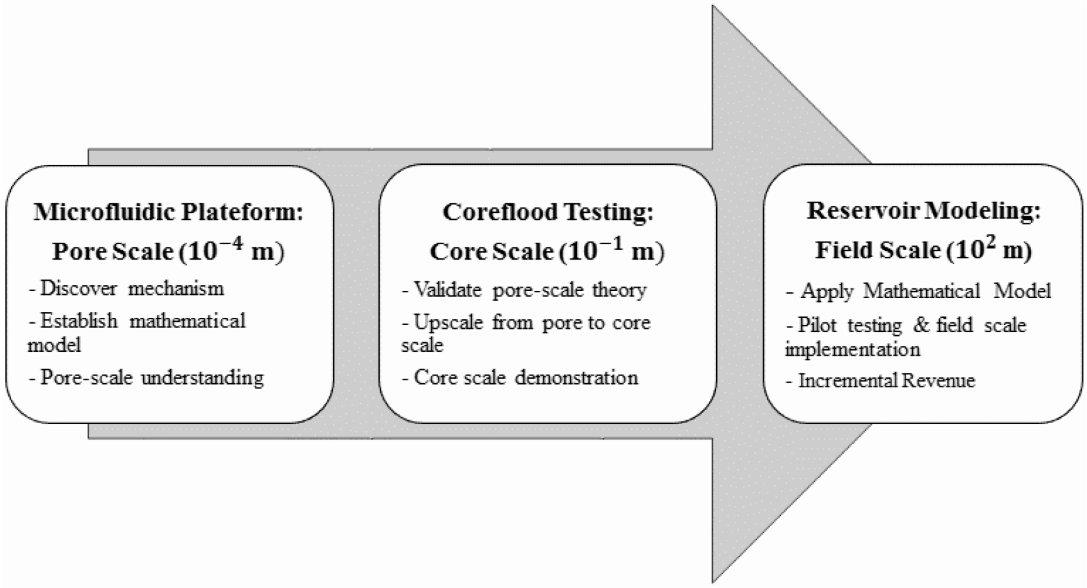


**Figure 1—Schematic flow diagram for multi-scale Nano-EOR.**

## Experimental Procedure

### Materials

Spherical shaped hydrophilic silica nanoparticle (HSN) was used in this study. Artificial sea water (ASW) was used as brine phase. ASW was prepared in the laboratory by mixing salts in de-ionized water to obtain the following composition (grams/kg): $Na^{+}$ 10.764, $K^{+}$ 0.387, $Ca^{2+}$ 0.406, $Mg^{2+}$ 1.297, $HCO_3^{-}$ 0.142, $Br^{-}$ 0.066, $Cl^{-}$ 19.353, $SO_4^{2-}$ 2.701 and $H_3BO_3$ 0.026. Light sweet crude oil (API:28, Viscosity: 5 cP@80 °C) was used as model crude oil in the study for microfluidics and core-flooding experiments. Idaho Gray core sample was purchased from Kocurek industries and was used in the core-flooding experiment.

### Method

***Nanoparticle Size and Zeta-potential measurements.*** The particle size and zeta-potential measurements were conducted on a Malvern Zetasizer instrument using dynamic light scattering and laser Doppler micro-electrophoresis techniques. A cuvette containing the HSNs suspension was placed in the sample chamber of the instrument. In the suspension, particles move randomly due to the Brownian motion. DLS measures the diffusion of particles and convert it into particle size and particle size distribution using the Stokes-Einstein equation. For zeta-potential measurement, HSNs suspension filled in the folded capillary cell was placed in the instrument sample compartment where electric field was applied through it. Nanoparticles in the presence of electric field moved with the velocity which was related to their zeta-potential. Instrument by means of phase analysis light scattering measured velocity and used velocity to calculate zeta-potential. Mean diameter and zeta-potential was measured as 15 nm and (-)32 mV respectively.

***Microfluidics Setup Design and Experimental Procedure.*** Microfluidics set up consisted of syringe pumps, microscope equipped with camera and light source, a low range sensitive transducer, syringes, tubing, connectors and micromodels. Two different micromodels called dead-end pore microchannel and 2.5 D micromodel were used in the microfluidics experiments.

***Dead-End Pore Microchannel Design and Experimental Procedure.*** Pore scale crude oil recovery experiment was conducted on dead-end pore microchannel. Dead-end pore glass microchannel consisted of pores connected to a main channel through a 3-D throat. The pore diameter was 230 μm and the width of throat was 33 μm, and the minimum depth of throat was 6 μm (Figure 2a). The experiment protocol very similar to a typical crude oil recovery experiment was used. Initially crude oil was injected through the syringe pump to saturate entire main channel and both the dead-end pores completely with the crude oil. Aqueous phase at very low flow rate (0.1 ml/hr) was injected to displace the crude oil in the main channel and to trap crude oil in dead-end pores (Figure 2a). Following this, HSNs suspension at 0.1ml/hr was injected into the main channel and the trapped crude oil's evolution during the HSNs injection was captured by microscope. Picture of the captured during the experiment is shown in Figure 2b.

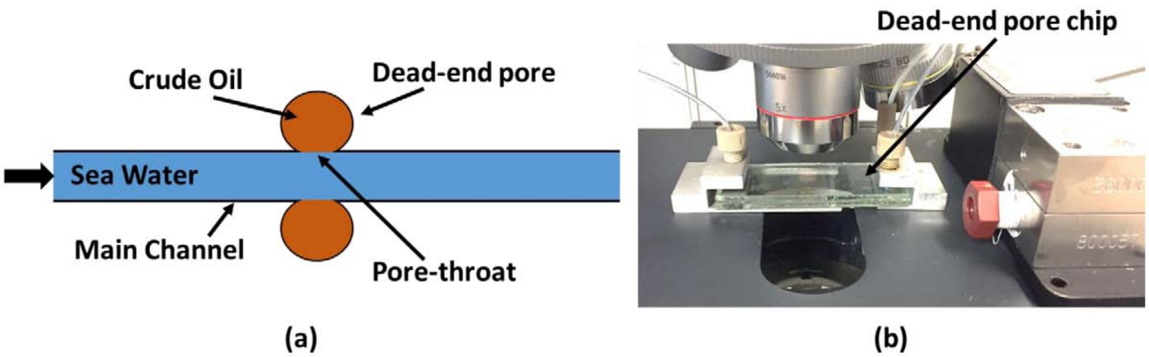


**Figure 2—Images of the microscopic visualization setup. (a) Conceptual line diagram of the dead-end pore microchannel. (b) Dead-end pore microchannel during experiment.**

***Porous Micromodel (2.5 D reservoir-on-chip) Design and Experimental Procedure.*** Porous micromodel was consisted of 2-D arrangement of 104 interconnected 3-D pores in a glass framework as reported by Xu et al.[15,16]. Each pore in this micromodel comprised of pore body and four pore throats. The depth of pore bodies was 22 μm each of which was connected to the four nearest neighboring pore-throats each of which having 6 μm depth and 33 μm width. The distance between the center of neighboring pores was 200 μm. Total pore volume was 4.4 μl and the liquid permeability as measured on microfluidics setup was 1100 mD. The fluid injection sequence was very similar to the one used for dead-end pore microchannel experiment. Initially, micromodel was saturated with seawater which was displaced by injecting crude oil at flow rate of 9 μl/hr (4 ft/day) to achieve connate water and initial crude oil saturation in the pores. ASW at this point was injected at flow rate of 9 μl/hr (4 ft/day) as secondary flooding agent to displace crude oil. ASW injection displaced crude oil from the pores towards the outlet. ASW injection was intentionally done for longer duration to make sure crude oil was no longer recovered at the outlet. HSNs suspension was injected at this stage to displace crude oil which was not recovered from the micromodel during prolonged ASW injection. Images from top was captured at regular intervals throughout the injection process and were analyzed on open source Image-J software to determine amount of crude oil and ASW present in the micromodel, which was used to calculate % oil recovery as a function of time during the experiment.

***Coreflooding Setup Design and Experimental Procedure.*** Core-flooding setup consisted of a hydrostatic core holder for confining core sample, a vacuum pump for removing air from the core, floating piston accumulators and injections pumps for injecting ASW, crude oil and HSNs fluids into the core, mineral oil pump for applying overburden pressure, and a fraction collector for collecting outlet samples at regular intervals. Idaho Gray core sample was used for coreflooding experiment. The core sample external surface was thoroughly cleaned in running deionized water and dried in the oven at 100 °C to evaporate all the water until weight of the dried cores stopped changing. Dried cores were scanned on X-ray CT scanner in order to visualize core internals and make sure they are free of any abnormal defects, cracks, vugs and non- homogeneity. Following cleaning, core sample was placed in the core holder, overburden pressure was applied and air was removed from the core. Effective pore volume (PV) was measured by injecting ASW in the core using fluid re-saturation method (Pore Volume = Fluid Injected – Fluid Collected – Dead Volume). For the permeability of the core, differential pressure across the core was measured for different flow rates of ASW through the core. Darcy's equation ($q= (k*A*\Delta p)/(\mu*L)$) was used in which flow rate and differential pressure are connected through core permeability. In this equation, q is injection flow rate, k is permeability of the core sample, A is cross section area, Δp is the differential pressure across the core, μ is viscosity of fluid and L is length of the core sample. Following porosity and permeability measurement, crude oil was injected into the core until irreducible water saturation level is reached. Remaining amount of aqueous and oil phase in the core was determined to calculate initial crude oil and water saturation in the core. Oil saturated core was left for 24 hours for oil droplets to reach equilibrium. ASW was used during water flooding phase followed by tertiary recovery phase during which HSNs suspension prepared in ASW was injected to displace crude oil. Recovered oil and ASW was measured using graduated cylinder and plotted as % of initial oil in the core.

## Results & Discussion

**Understanding of Mechanism in the Dead-End-Pore Microchannel**

Crude oil was trapped the dead-end pores. Some of the crude oil was also seen present on the channel walls. 5 wt% HSNs suspension in DI water was injected in the dead-end pore microchannel to recover crude oil trapped inside the two dead-end pores. Interestingly, during the injection of HSNs suspension, it was observed that crude oil in the pores swelled considerably and snapped-off into the main channel in the form of oil drops (shown in Figure 3a). The crude oil present on the main channel surface also swelled very significantly, and ultimately removed from the surfaces and progressed left-to-right with the flow in the main channel (as shown in Figure 3a). It was also observed that the crude oil affinity changed from wetting to non-wetting phase on the glass surface. Change in wetting behavior was more evident on the main channel, where crude oil initially in the shape of film was transformed to more like expanding drops which indicated significantly increased crude oil contact angle with the glasss surface. In the dead-end-pores, the HSNs suspension was observed to be progressing inward in the two phase (crude oil – glass surface) region forming three phase region (crude oil – glass surface – aqueous phase). The three phase interface inward movement could be due to the formation of a nanoparticle layer in between glass and crude oil, much like an inward moving wedge, which was also observed by Wasan et al. with a theory of disjoining pressure[10,11]. Overall phenomena possibly could be disjoining pressure driven wettability alteration along with crude oil swelling. Snapshots of microchannel shortly after injection of nanoparticles (after 0.1 hours) and during the injection (after 6 hours) and towards the end of injection (after 48 hours) are shown in Figure 3a. One of the dead-end-pore was observed under the microscope after 23 hours. Many tiny water droplets were observed inside the oil bulk, which explained crude oil swelling. These tiny droplets coalesced to form bigger droplets which were observed close to oil-water interface at the pore throat. We defined this new system as a water-in-oil-in-water double emulsion (Figure 3b).

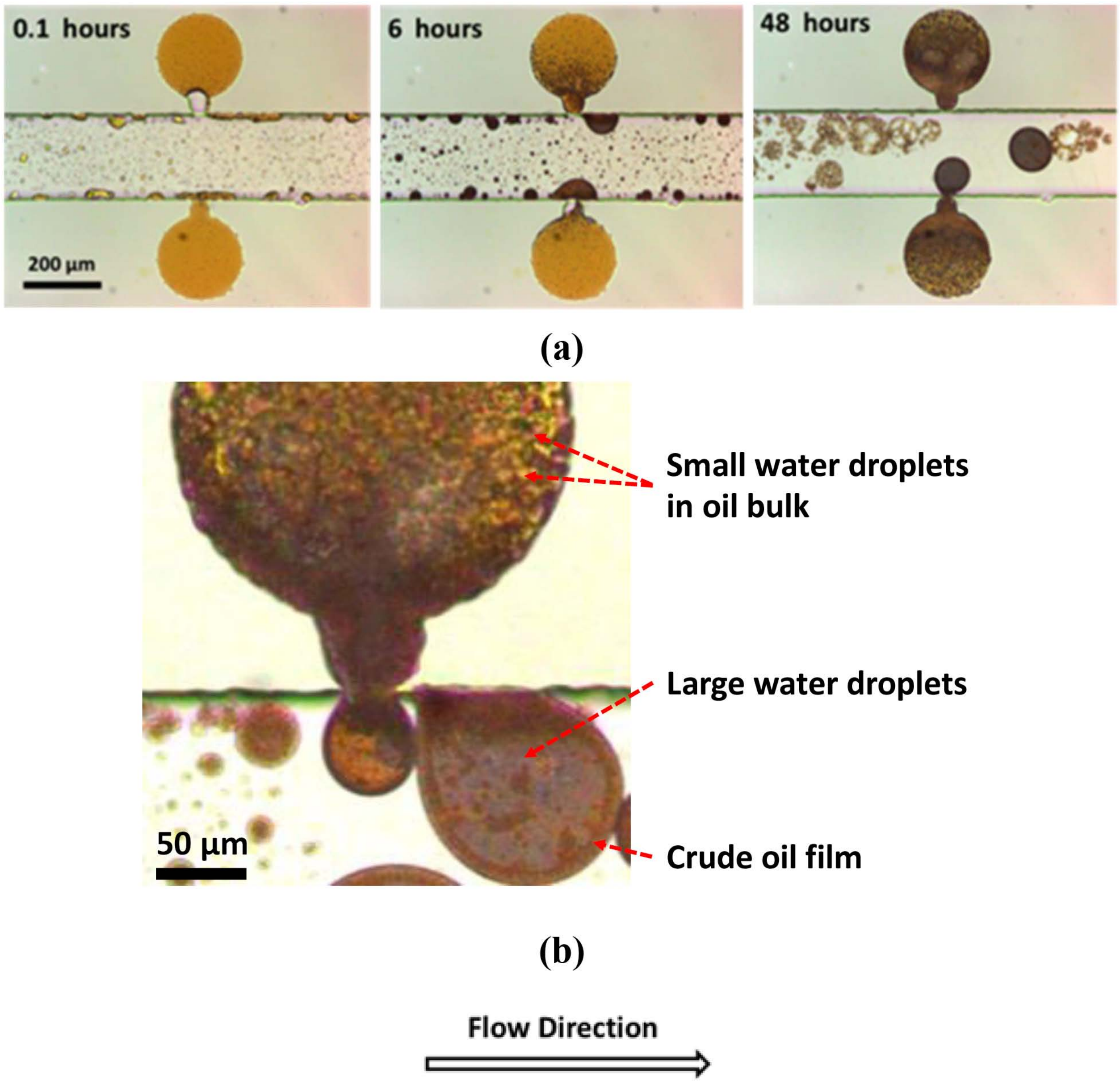


**Figure 3—(a) Snap shot of trapped crude oil in microchannel at 0.1 hours, 6 hours and 48 hours (b) Zoomed-in observation of swelled crude oil after 23 hours.**



## HSNs Suspension Flooding in the Reservoir-on-a-Chip 2.5-D Micromodel

Following the crude oil swelling observed on the dead-end-pore micromodel, oil recovery experiment was conducted on the 2.5-D micromodel. In the case of dead-end-pore micromodel experiment, concentrated HSNs suspension (5 wt%) was prepared in de-ionized water, however in the case of 2.5-D micromodel, comparatively diluted HSNs suspension at 2000 PPM concentration prepared in ASW was used as the tertiary injection fluid. ASW was used during secondary water flooding. The goal was to identify if there is any advantage of observed crude oil swelling phenomenon in crude oil recovery. Transparent micromodel allowed us to visualize oil displacement under the microscope. Snapshots during the injection process were recorded on the Nikon SLR camera are shown in the Figure 4a. Top-left image was taken initially when the micromodel was saturated with the crude oil with irreducible water distributed all over the chip in very small amount. In the picture, crude oil phase is marked dark yellow in color and anything other than dark yellow is ASW phase or emulsion of crude oil and ASW phase. Top right image is captured when system achieved steady state after two hours of ASW flooding. As expected, viscous fingering was observed and at the end of ASW flooding, significantly large area of the chip was not swept at all which resulted in the significant portion of the crude oil not recoverd from the chip. Bottom left image is captured during HSNs suspension flooding and bottom right image was captured at the end of HSNs flooding. It was clearly visible that HSNs suspension injection mobilized significant amount of crude oil from the un-swept region. Almost no change in crude oil saturation was observed in the swept region indicating that HSNs suspension did not affect residual crude oil. Similar to the dead-end-pore micromodel, tiny droplets of water were observed in the crude oil phase along with crude oil de-wetting as shown in the Figure 4b. Generation of water droplets in the crude oil phase in this case was much lesser which was probably not adequate enough to recover any significant amount of crude oil from the swept region. Overall, observations on the 2.5 D micromodel was found to be very consistent with the observations on the dead-end-pore micromodel.

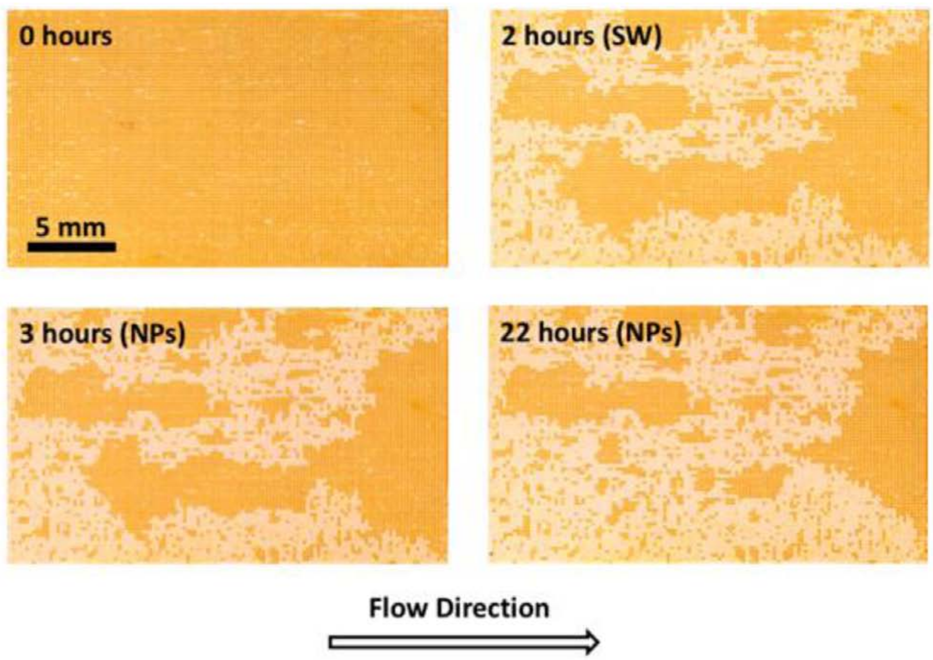


(a)

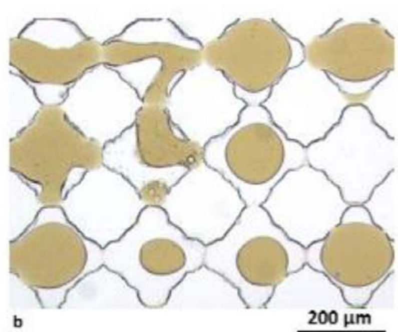


(b)

**Figure 4—(a) Original images of micromodel flooding at different time (b) Microscopic image of swept region after 2000 ppm negatively charged NPs suspension in ASW flooding.**

From the image analysis, quantification of crude oil recovered during ASW flooding and HSNs flooding was made and the recovery curve is shown in the Figure 5. As shown in Figure 5, crude oil recovery during the ASW flooding was about 33%. Injection of 2000 PPM HSNs in ASW after secondary crude oil after ASW flooding didn't recover any significant amount of crude oil for several hours but after coule of hours HSNs suspension started to produce crude oil from the un-swept region. It appears that the crude oil swelling required several hours to occur as was observed during dead-end-pore micromodel experiment, and which then helped to divert injected HSNs suspension towards the regions which were un-swept during ASW flooding. The time scale for slow incremental crude oil recovery corresponded very well with the crude oil swelling and ultimately recovery observed on the dead-end-pore microchannel. Overall, 11.8 % incremental oil was recovered during HSNs suspension flooding. From this experiment, we confirmed 2000 PPM concentration of HSNs in ASW enhanced crude oil recovery due to improving sweep efficiency and not by reducing residual oil saturation.

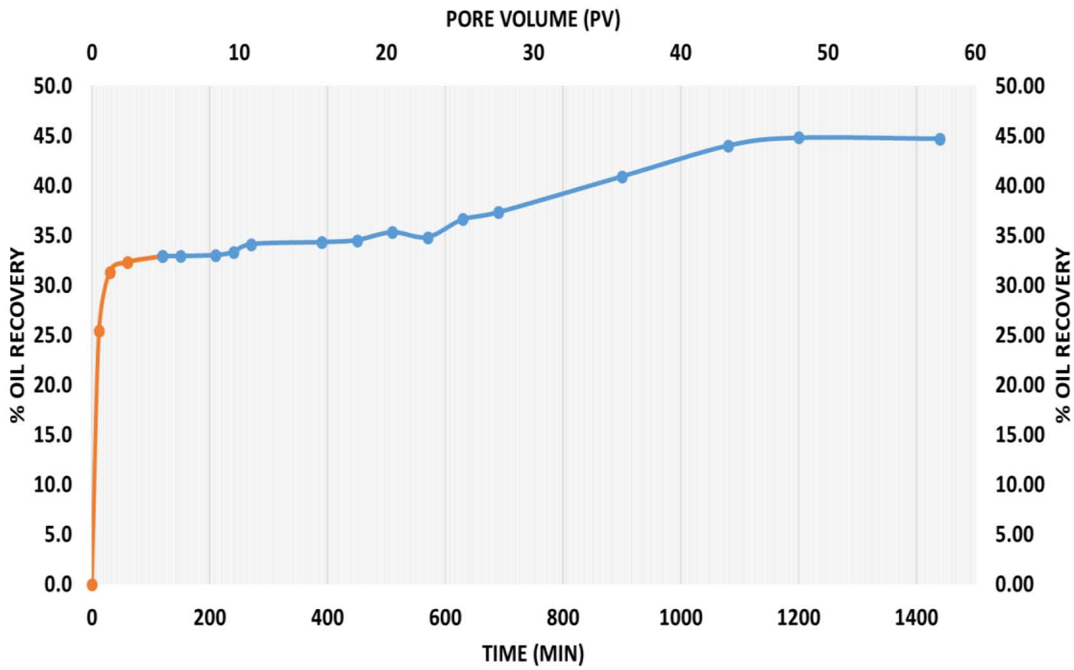


**Figure 5—% Oil recovery during injection of ASW (orange), 2000 ppm HSNs suspension in ASW injection (blue) as a function of time (primary x-axis) and pore volume collected (secondary x-axis) during the reservoir-on-a-chip experiment.**

## HSNs Flooding Through Idaho Gray Core on Coreflooding Setup

HSNs suspension prepared in ASW was evaluated for oil recovery on core-looding setup to find out if the findings from micromodels can be applied at the core scale. Coreflooding experiment was conducted on the light and sweet crude oil saturated high permeability Idaho Gray core. Core was dried, vacuumed and then saturated with ASW and the pore volume was measured and porosity was calculated. Following this, ASW was injected in the core and differential pressure at different flow rate was measured to calculate the permeability. Details of the experiment is summarized in the Table 1 below.

**Table 1—Summary of the core-flooding experiment.**

| Idaho Gray Core Specifications | |
|---|---|
| Orientation | Vertical |
| Dry Weight | 299.5 grams |
| Dimensions | Len. 6" & Dia. 1.5" |

| Injection Fluids | |
|---|---|
| Crude Oil | Light and sweet crude oil |
| Water Flooding | Artificial Sea Water |
| EOR Flooding | 5000 PPM HSNs in ASW |

| Idaho Gray Core Properties | |
|---|---|
| Pore Volume | 38.1 mL |
| Porosity | 22.3 % |
| Permeability | 1513 mD |

| Process Conditions | |
|---|---|
| Flow Rate | 0.4 mL/min |
| Temperature | 25 °C |
| Overburden Pressure | 1000 psig |

Crude oil injection was started in vertical orientation from the bottom to top and core was saturated with crude oil. Crude oil displaced ASW present in the core. Initially only aquous phase was collected at the outlet. Crude oil injection was continued until there was no ASW collected at the outlet and only100% crude oil was collected at the outlet. Amount of crude oil and ASW present inside the core was calculated using mass balance. Following this, ASW flooding was started and the crude oil was displaced. Initially only, crude oil was collected at the outlet and afterward ASW breakthrough occurred before one pore volume. Following ASW flooding, 5000 PPM HSNs suspension in ASW was injected in the core and the recovered crude oil was collected at the outlet. The cumulative % oil recovery with time and pore volume is plotted in Figure 6. As it can be seen in the Figure 6, the % oil recovery during ASW flooding was 57.1% which went up by 19 % to 76.1% during HSNs suspension injection. Interestingly, HSNs suspension showed slow and incremental oil recovery and the obtained oil recovery curve is very similar to the one observed for 2.5 D micromodel confirming pore-scale and pore-network studies conducted in the micro-models co-related well with the coreflooding results.

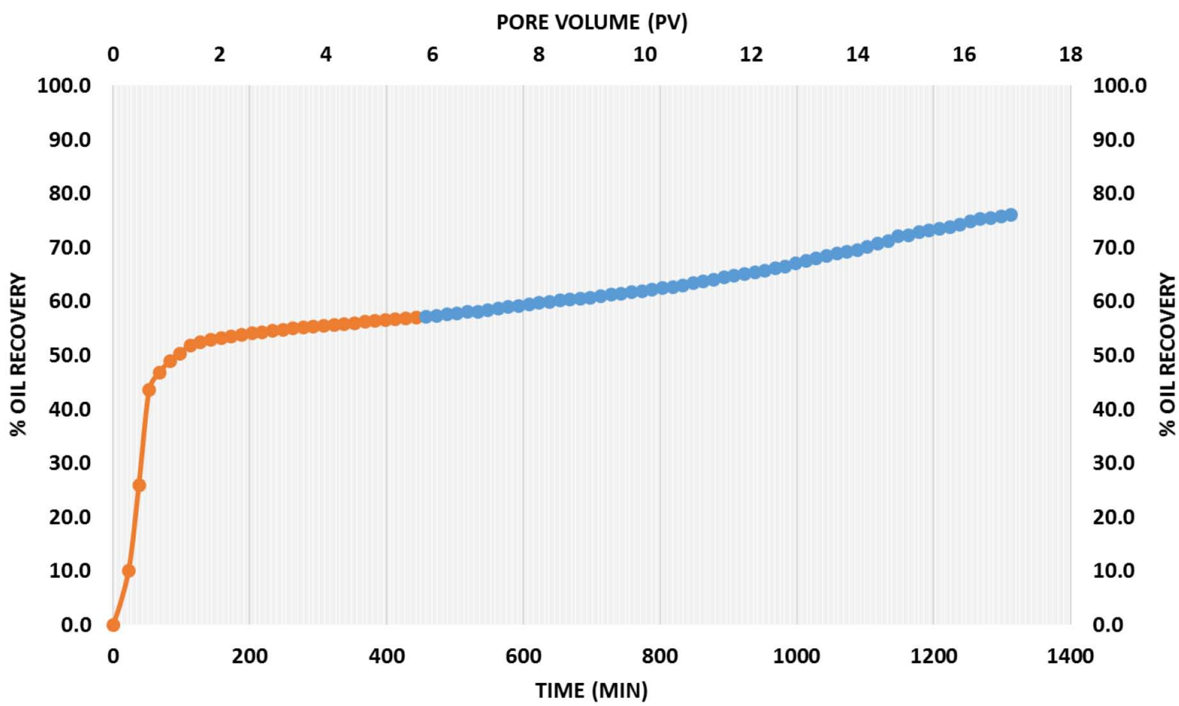


**Figure 6—% Oil recovery during injection of ASW (orange), 5000 ppm HSNs suspension in ASW injection (blue) as a function of time (primary x-axis) and pore volume collected (secondary x-axis) during the coreflooding experiment.**

## Conclusions

A dead-end-pore microchannel was applied to study the trapped oil's interaction with HSNs aqueous suspensions. Swelling of crude oil was observed during HSNs suspension injection, which was caused by spontaneous generation of aqueous droplets in crude oil. Such swelling crude oil was also investigated on 2.5-D micromodel flood experiment, and showed excellent conformation control performance that provided 11.8% incremental oil recovery. It was found that HSNs did not change the residual oil saturation, but improved sweep efficiency. Conformance improvement was induced by swelling oil's occupation of swept water channels. Oil recovery curve from micromodel flood experiment co-related with the coreflooding data. In both cases, incremental oil recovery came slowly and continuously in over twenty hours.

Compared to coreflooding experiment, micromodel flooding can provide more in-situ and dynamic saturation information, with much less cost in time and money. Micromodel flooding could be treated as an efficient and significant supplement to core-flooding. Ultimate outcome of pore scale to core scale understanding is extremely beneficial in connecting pore scale mechanism with the core scale performance and finally applications in the reservoir simulation and successful field implementation.

## Acknowledgements

We would like to sincerely thank Baker Hughes, a GE Company (BHGE) for financially supporting and allowing us to publish this work. We would also like to thank Dr. Matthew T. Balhoff and his reseresearch groups' from the University of Texas at Austin for technical support in building up micromodel experiment setup, Noel F. Atzmiller from BHGE for proofreading the manuscript, and our collegues' miscellaneous help in the laboratory.

## References

https://www.iea.org/oilmarketreport/omrpublic/

https://www.rigzone.com/training/insight.asp?insight_id=313

https://www.energy.gov/fe/science-innovation/oil-gas-research/enhanced-oil-recovery

Gurgel, Alexandre & Moura, Maria & Castro, Tereza & L BarrosNeto, E & Dantas Neto, Afonso. (2008). A review on chemical flooding methods applied in enhanced oil recovery. *Braz. J. Pet. Gas*. **2**. 10.5419/bjpg.v2i2.53.

Pal, S., Mushtaq, M., Banat, F. et al. *Pet. Sci.* (2018) **15**: 77. https://doi.org/10.1007/s12182-017-0198-6.

Chegenizadeh Negin, Saeedi Ali, Quan Xie, Most common surfactants employed in chemical enhanced oil recovery, *Petroleum*, Volume **3**, Issue 2, 2017, Pages 197–211, ISSN 2405-6561.

Puskas, S., Vago, A., Toro, M., Ordog, T., Kalman, G., Hanzelik, P., … Lakatos, I. (2018, March 26). *Surfactant-Polymer EOR from Laboratory to the Pilot*. Society of Petroleum Engineers. doi:10.2118/190369-MS.

Finol, J., Al-Harthy, S., Jaspers, H., Batrani, A., Al-Hadhrami H., van Wunnik, J.N.M., Stoll, W.M., Faber M.J., and de Kruijf, A. (2012). "Alkali-Surfactant-Polymer Flooding Pilot Test in Southern Oman". SPE-155403.

Barnes, J.R., Dirkzwager, H., Smit, J., Smit, J., On, A., Navarrete, R.C., Ellison, B, Buijse, M.A., (2010). "Application of Internal Olefin Sulfonates and Other Surfactants to EOR - Part 1: Structure - Performance Relationships for Selection at Different Reservoir Conditions", SPE-129766, doi:10.2118/129766-MS.

Wasan, D. T.; Nikolov, A. D., Spreading of nanofluids on solids. *Nature* 2003, **423**, 156–159.

Nikolov, A.; Kondiparty, K.; Wasan, D., Nanoparticle self-structuring in a nanofluid film spreading on a solid surface. *Langmuir* 2010, **26**, 7665–7670.

Katherine R. Aurand, Gunnar Sie Dahle, and Ole Torsæter, COMPARISON OF OIL RECOVERY FOR SIX NANOFLUIDS IN BEREA SANDSTONE CORES, International Symposium of the Society of Core Analysts held in Avignon, France, 8-11 September, 2014.

Chegenizadeh Negin, Saeedi Ali, Quan Xie, Application of nanotechnology for enhancing oil recovery – A review, *Petroleum*, Volume **2**, Issue 4, 2016, Pages 324–333, ISSN 2405-6561.

Suresh, R., Kuznetsov, O., Agrawal, D., Darugar, Q., & Khabashesku, V. (2018, April 30). Reduction of Surfactant Adsorption in Porous Media Using Silica Nanoparticles. Offshore Technology Conference. doi:10.4043/28879-MS

Xu, K.; Bonnecaze, R.; Balhoff, M., Egalitarianism among Bubbles in Porous Media: An Ostwald Ripening Derived Anticoarsening Phenomenon. *Physical review letters* 2017, **119** (26), 264502.

Xu, K.; Liang, T.; Zhu, P.; Qi, P.; Lu, J.; Huh, C.; Balhoff, M., A 2.5-D glass micromodel for investigation of multi-phase flow in porous media. *Lab on a Chip* 2017, **17** (4), 640–646.